Journal of Structural Geology, Vol. 10, No. 7, pp. 707 to 715, 1988
Printed in Great Britain

0191-8141/88 $03.00 + 0.00

Factors affecting the kinematic interpretation of asymmetric boudinage in shear zones

ARTHUR G. GOLDSTEIN

Department of Geology, Colgate University, Hamilton, NY 13346, U.S.A.

(*Received* 7 *May* 1987; *accepted in revised form* 20 *June* 1988)

Abstract—Based on work along a major mylonite zone in the northern Appalachians and scale model studies, a new mechanism for the origin of asymmetric boudins in shear zones is proposed. Along the Honey Hill Fault in southern Connecticut, granitic sills intruded into calc-silicate gneisses and schists were oblique to the boundaries of the mylonite zone and experienced the following sequence in the production of sigmoidal boudins: (1) as the calc-silicate schists experienced mylonitization and flow, the more competent, coarse-grained granitic sills deformed by extensional fracturing and quartz veining; (2) continued extension of granitic sills was accommodated by 'normal' shear on early-formed quartz veins; (3) continuing extension of sills and ductile modification of the corners of boudins resulted in granitic 'fish' with tails which stream from the top of the boudin in the 'down-dip' direction and from the bottom in the 'up-dip' direction. Based on a variety of kinematic indicators, the sense of asymmetry of the tails is identical to that expected for recrystallization tails on sheared augen (σ structure). Models composed of silicone putty and Plasticine were created to investigate the effect of pre-shearing geometry on boudin evolution, and were deformed in a simple shear device. The models reproduce the kinematics deduced from field relations and suggest that one of the primary factors in controlling the amount of extension is the angle which early veins make with the shear zone boundary. Varying the angular relationships in the models suggests that other pre-shearing geometric factors may affect the geometry of boudins formed in this way. Boudins formed through this mechanism appear very similar to Hanmer's type II asymmetric boudins. Because the pre-shearing geometry can exert a control on boudin asymmetry, caution should be used when attempting to deduce shear sense or shear strain values from asymmetric boudinage.

INTRODUCTION

WHEN competent layers in a ductile matrix are extended parallel to their length, they commonly extend discontinuously. The resulting structures are dependent on the competence contrast and range from fracturing of the competent layer at high competence contrast to pinch and swell at lower contrast. At high strains the competent layer may become separated into either angular blocks which experience ductile modification of their corners, or elliptical pods (Cloos 1947, Rast 1956, Ramsay 1967). Mechanically the two phenomena are distinct in that the first results from brittle failure and the second from ductile elongation. Symmetrical boudinage, in which the direction of extension is roughly parallel to the layering, has been treated both analytically and experimentally (Ramberg 1955, Strömgård 1973, Smith 1975, 1977, Fullager 1980, Lloyd & Ferguson 1981, Lloyd *et al.* 1982). The analysis of asymmetrical boudinage, in which the direction of extension is oblique to the layering, has been treated theoretically by Strömgård (1973) and special reference to the modification of pre-existing boudins by simple shear has been treated by Ghosh & Ramberg (1976) and Hanmer (1986). The purpose of this paper is to describe another mechanism for the formation of asymmetrical boudinage which occurs in shear zones and is different from that proposed by Ghosh & Ramberg (1976) and Hanmer (1986). Specifically, Hanmer (1986) has described two types of asymmetric boudinage which he refers to as type I and type II, which result from shape modification of pre-shearing boudins. The boudinage described in this paper results from rotation of fracture-bounded blocks and will be referred to as type III boudinage (Fig. 1). It will be shown, based on field and experimental results, that it may be very difficult to differentiate between type II and type III asymmetric boudinage and that type III asymmetric boudinage may be very difficult to utilize as an independent kinematic indicator.

FIELD RELATIONS

Very large roadcuts in southern Connecticut (Fig. 2) reveal an unusual form of boudinage. Sills of granitic

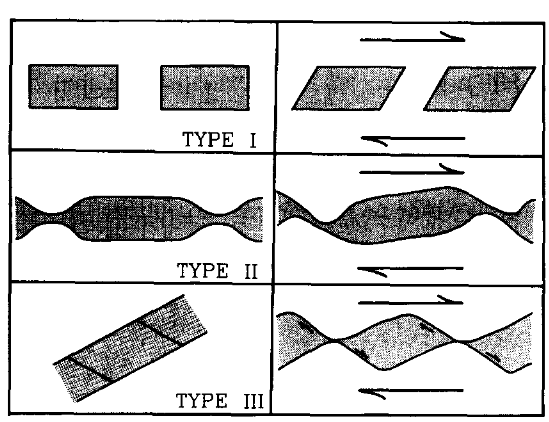

Fig. 1. Three types of asymmetric boudinage which may develop in shear zones. Type I and II asymmetric boudinage, proposed by Hanmer (1986) require the existence of either blocky or pinch and swell boudins prior to shearing. Type III asymmetric boudinage, proposed in this paper, requires that layering be inclined to the shear zone and lie in the extensional field.

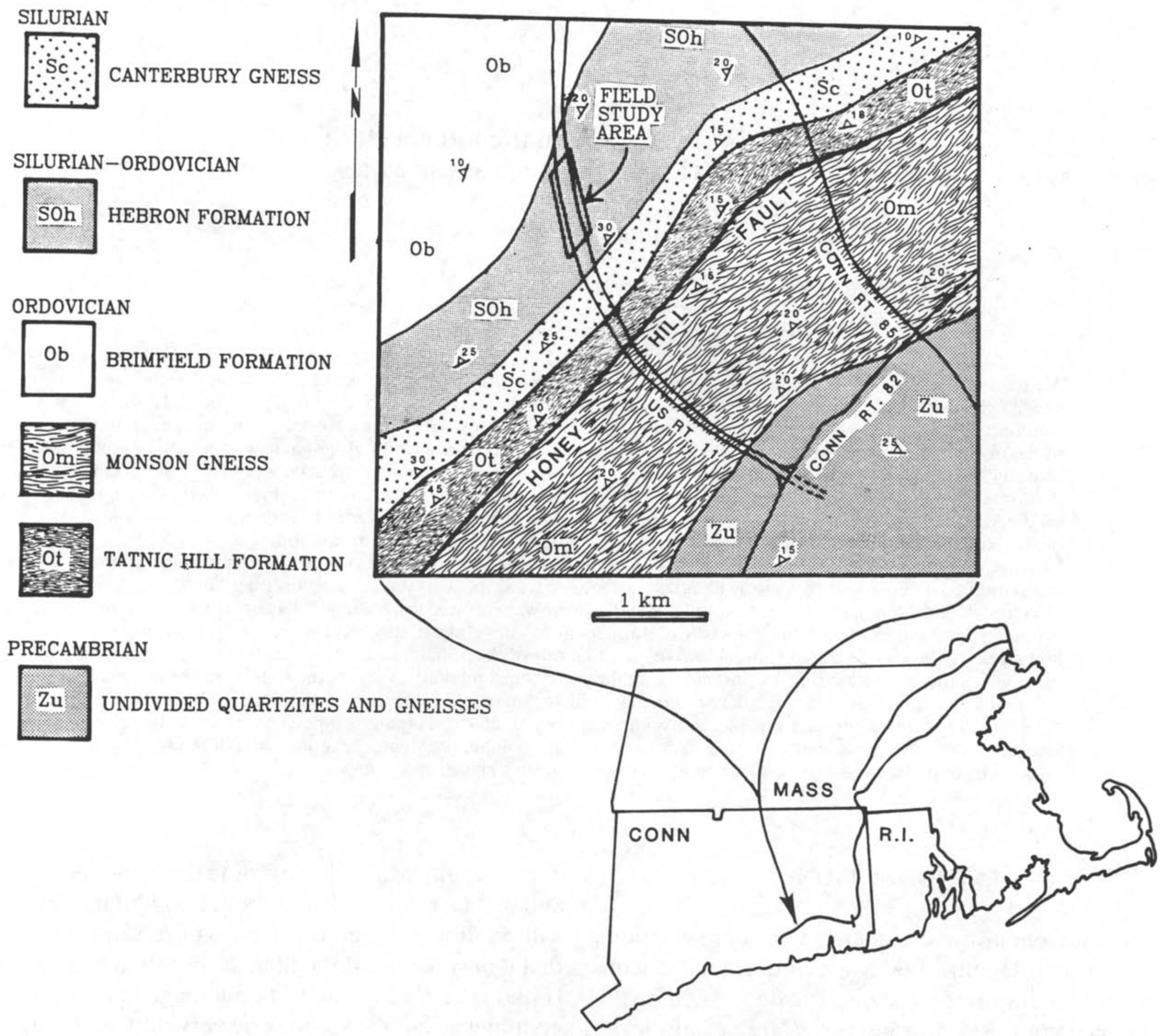

Fig. 2. Map of southern New England showing the locations of faults which dip to the north and west and the location at which the asymmetric boudinage has been observed.

material that were intruded into calc-silicate gneiss and schist have been dismembered such that they exhibit asymmetric 'tails' similar to the asymmetric recrystallization tails (σ structure) on feldspar augen (Simpson & Schmid 1983). The locality lies within the Honey Hill mylonite zone in the northern Appalachians (Fig. 2) which is part of a major terrane-bounding fault system in the northern Appalachians and has had a long and complex history of motions. The earliest recognizable period of motion is Silurian (Dixon 1982, Goldstein 1986) and is characterized by left-lateral displacement with a thrust component. The next period of motion occurred during the Permian Alleghanian (Hercynian) orogeny (O'Hara & Gromet 1983) and is characterized by oblique normal motions with a northwestern vergence (Goldstein 1982, Goldstein & Owens 1985). This late Paleozoic phase of motion was sufficiently intense along the Honey Hill fault to completely obliterate all traces of the earlier motions. The asymmetric boudinage discussed below is related to the later phase of motion.

Mesoscopic geometry

The locality described here lies approximately 2.5 km north of the surface trace of the Honey Hill Fault (Fig. 2) and approximately 1.0 km structurally above the fault trace. The orientations of foliation, mineral elongation lineation and intrafolial folds as well as microstructural shear sense indicators at the locality are similar to those in other regions of the mylonite zone. Within the gently NW-dipping calc-silicate schists and gneisses of the Siluro-Ordovician Hebron formation, a strong mineral elongation lineation plunges toward the northwest (Fig. 3). The lineation is composed of aligned hornblende crystals, biotite streaks and quartz rods. Microstructurally, the schists are composed of heterogeneously grain-size-reduced aggregates of biotite, hornblende, actinolite, quartz, plagioclase and, in some samples, sphene or calcite. Within the finest grained portions, clasts of plagioclase, hornblende and actinolite are surrounded by a very fine-grained matrix of biotite, quartz and calcite with an *S–C* fabric. The geometry of the *S* and

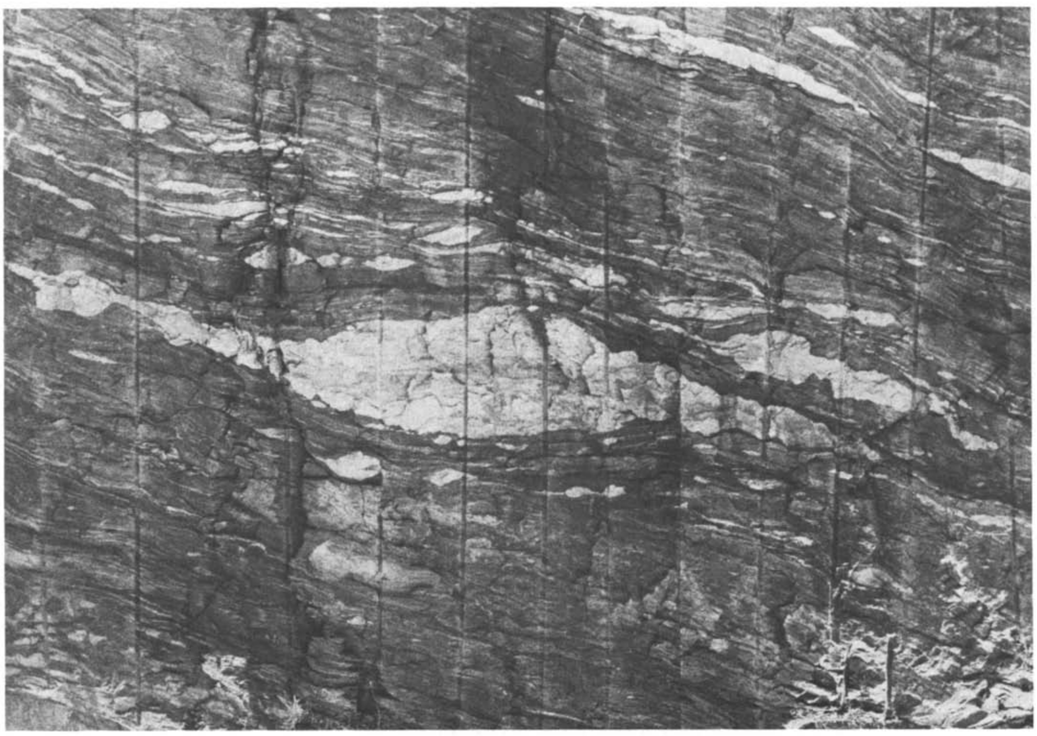

Fig. 4. Photograph of large asymmetric boudinage viewed looking WSW. The orientation of mineral elongation lineations is subparallel to the direction of the roadcuts. The sense of asymmetry of all boudins is the same with the 'tails' streaming 'down-dip' from the top of the boudins and 'up-dip' from the bottom. Tails lie nearly parallel to the overall trend of foliation and the 'body' of the boudins is back-rotated. Drill holes are approximately 1 m apart.

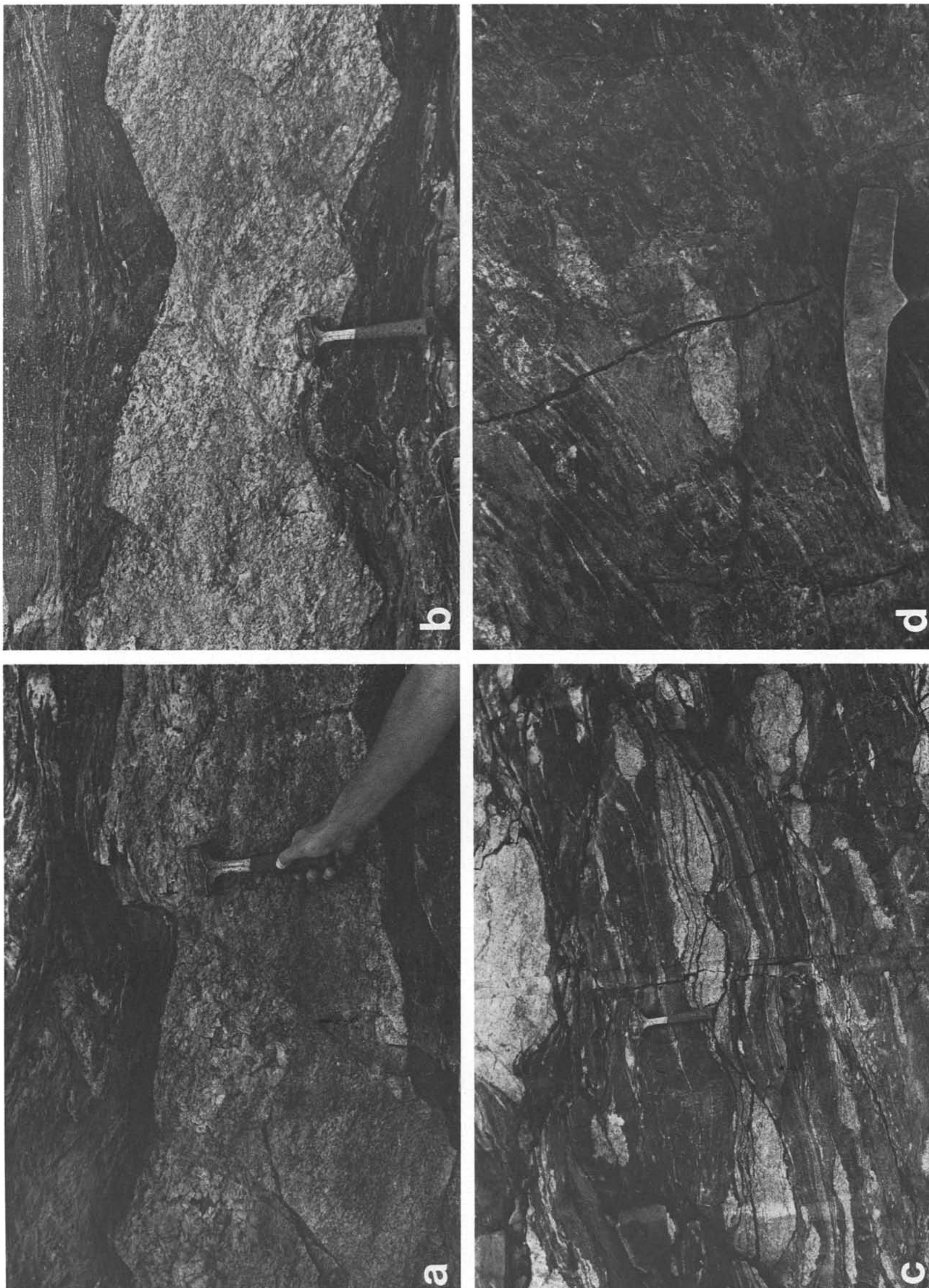

Fig. 5.

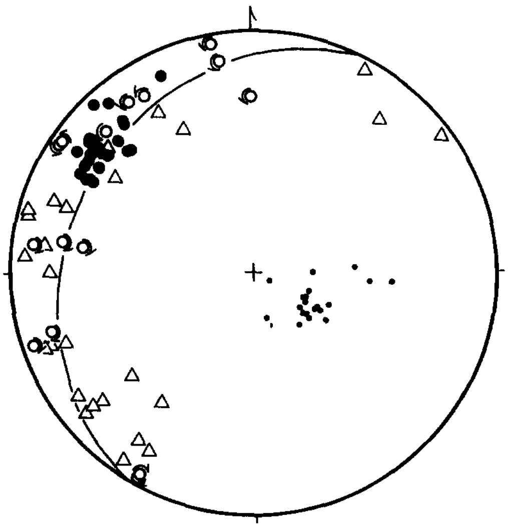

Fig. 3. Lower-hemisphere, equal-area projection of structural elements measured at the field locality. Fold axes are shown with the fold rotation sense when viewed in the down-plunge direction and boudin axes are defined as the local line of intersection between the edge of the boudin and the enclosing foliation.

C surfaces define low-angle normal motion as do rotated porphyroclasts and asymmetric pressure shadows. Additional evidence for low-angle normal motion is the geometry of mesoscopic intrafolial folds which have a separation angle geometry (Hansen 1971) with respect to the elongation lineation (Fig. 3). Low-angle normal motion has been documented at numerous other localities along the Honey Hill and Lake Char Faults (Goldstein 1982, Goldstein & Owens 1985).

Asymmetric boudins are developed from granitic sills and range from several cm to several m in thickness and width. Mapping of very large boudins (>10 m length) suggests that some boudins are elongate at a high angle to the mineral elongation lineation and have shapes approximating elongate oblate ellipsoids. The boudins have asymmetric 'tails' which consistently stream from the 'top' of the boudins in the 'down-dip' direction and from the 'bottom' of the boudins in the 'up-dip' direction (Fig. 4). Isolated boudins generally have their 'tails' parallel to the orientation of foliation and their 'bodies' dipping less steeply and, thus, appear back-rotated with respect to the enclosing foliation (Fig. 4). The tails are composed of a fine-grained, dynamically recrystallized equivalent of the granitic material and pods and stringers of very fine-grained, recrystallized quartz.

The boudins are observed in various stages of development (Fig. 5). The earliest stage is the formation of quartz-filled fractures in the granitic sills (Fig. 5a) which show no evidence of shear and are thus interpreted as extension fractures. The extension fractures contain up to 10 cm of quartz infilling, do not penetrate into the country rock, are oblique to the layering at angles of approximately 70° and are regularly spaced. The quartz infilling is not fibrous and does not display any indication of being 'open-space' mineralization. The quartz-filled extension fractures have been utilized for later 'normal' sense displacement (Figs. 5a–c). The surrounding calc-silicate schists and gneisses indicate flow around the developing boudins. With increasing shear displacement on early-formed fractures, the boudins separated further (Fig. 5c) and became totally isolated from the other fragments of the original layer (Figs. 4 and 5d). The resulting fragments experienced ductile modification of their corners resulting in a sigmoidal shape with the tails lying nearly parallel to the foliation in the surrounding schists and foliation in the boudins inclined to the external foliation (Figs. 4 and 5d). Slip between blocks occurred during mylonitization of the enclosing schists and gneisses as evidenced by the parallelism in trend of lineations on the boudin-separating shears and in the mylonitized schists. Those shears with small displacement bear true slickenlines whereas those with larger displacement are decorated with quartz rods and biotite streaks. These observations suggest that small displacement shears began moving during the latest, coldest phases of motion on the Honey Hill Fault.

In the absence of additional data on shear sense, there are two interpretations of the origin of the boudins. One is to consider the 'normal' displacement between blocks as resulting from rigid-body rotation of individual boudins in response to shear with a thrust (southeastward) displacement. Such a model would require that, prior to shearing, layering was dipping in the same direction but more steeply than the shear zone boundary and that fractures were present before shearing and were inclined at high angles to the shear zone boundary. The boudins would rotate in harmony with the overall sense of shear and the sense of shear on the boudin-separating shears would be opposite to that of the zone (Cloos 1947, Wilson 1982). The second interpretation, which accounts for the boudin formation in the context of a normal component of shear, requires that prior to shearing layering was inclined less steeply than the shear zone boundary and that fractures were at a moderate angle to the shear zone boundary (Fig. 6). The non-parallelism between layering and the shear zone boundary is required by the extension of layering accommodated by 'normal' slip on boudin-separating shears which shows that layering lay in the field of extensional strain. Given such a geometry, the sense of displacement on boudin-separating shears would be in harmony with

Fig. 5. Photographs of asymmetric boudinage in the various stages of formation viewed looking ENE. The down-dip direction of foliation is to the left. (a) Initial stages of formation showing quartz-filled extension fracture with no displacement (left center) and small displacement on a parallel quartz-filled fracture. (b) Moderate displacement on extension fracture. (c) Asymmetric boudins which have become almost totally separated along sheared extension fracture. (d) Small asymmetric boudins which have been completely separated from the rest of the layer (compare with boudins in Fig. 4).

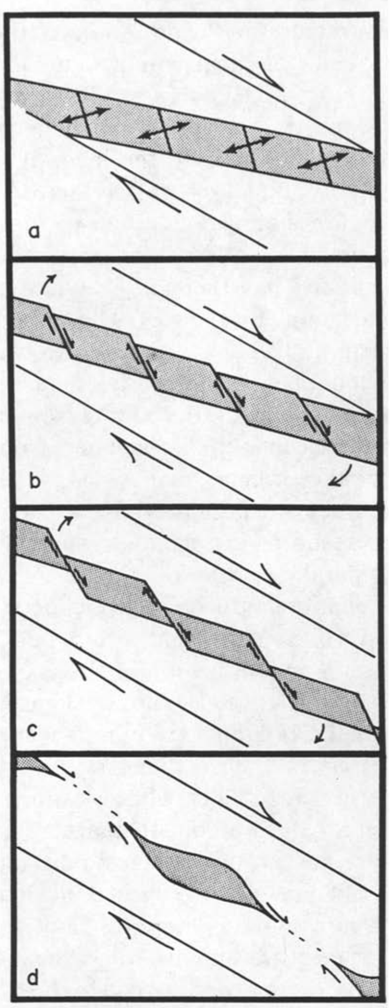

Fig. 6. Proposed model for the formation of the asymmetric boudins. (a) Layering begins nearly horizontal and extension is accommodated by formation of mode I fractures with mineral filling. (b) and (c) As shearing continues, layering rotates toward parallelism with the shear zone boundary and extension is accommodated by displacement on early-formed extension fractures. (d) At high shear strain values, boudins become completely separated and their corners experience ductile shape modification.

that of the overall shear zone. At high shear strains the enveloping surface of disrupted layering will be close to parallel with the shear zone boundary for either case, so to differentiate between the two interpretations, in the absence of independent shear criteria, would be difficult. For the locality illustrated here, independent shear sense indicators such as *C* and *S* structure, intrafolial folds (Fig. 2) and microstructures of a wide variety describe a shear sense with a normal component (Goldstein & Owens 1985). Thus, the second interpretation would be correct. This interpretation is similar in some respects to one proposed by Gaudemer & Tapponier (1987) but differs in the initiation of extensional shears as mode I fractures rather than shear planes and in the interpretation of the pre-shearing angular relationships.

MODEL STUDIES

Because the evolution of type III asymmetric boudinage in shear zones will be dependent on the pre-shearing geometry, a series of 32 models were constructed to test the effect of different geometric relationships on the development of type III asymmetric boudinage. The models were composed of blocks of Plasticine embedded in silicone putty and were separated by a thin film of putty to simulate fracture filling. The models, approximately 2 cm thick, contained a lower layer of putty approximately 0.5 cm thick to shield the Plasticine blocks from contact with the deformation apparatus. The models were placed in a shear box composed of vertical plexiglass sheets with a 2.5 × 11 × 10 cm well cut from the top which contained the models. No lubrication between the model and the deformation apparatus was introduced and the models were unconfined on their upper surface. A simple shear deformation was imposed on the models at a constant shear strain rate of 10^{-3} s^{-1} to a total shear strain of 1.73. Excellent cohesion

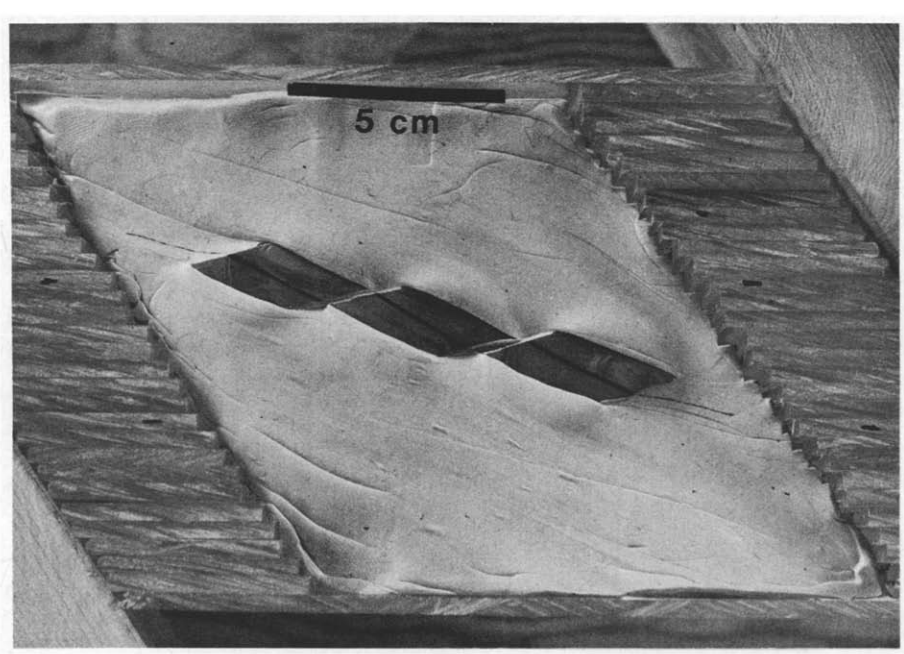

Fig. 7. Photograph of scale model deformed to shear strain of 1.73 (note that the passive line marker has rotated more than individual boudins.

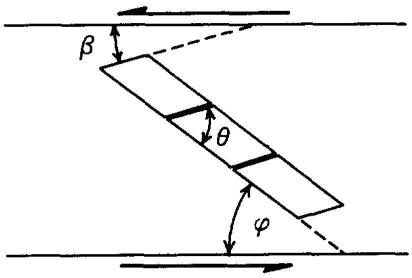

Fig. 8. System of notation used for geometry of model studies.

between the putty and Plasticine and the slow shear strain rate combined to prevent open spaces from developing at block margins, although some non-plane strain occurred (Fig. 7).

There are three geometric factors which could conceivably affect the form of type III asymmetric boudins: the angle which fractures make to the layering (θ); the angle which layering makes with the shear zone boundary (ϕ); and the angle which fractures make with the shear zone boundary (β) (Fig. 8). Only two of these angles are independent but the results of the model experiments, while not quantitatively significant, suggest that for a particular geometry, any one of the three angles (or the combined effect of the other two) could have an effect on the form of the rotated blocks.

Figure 9 shows the results of six experiments which illustrate the effect of the angle between the fractures and the shear zone boundary (β). Experiments are illustrated with layering inclined at 30, 50 and 10° to the shear zone boundary and with varying angles of fractures. Figure 9 shows that, for any orientation of layer-

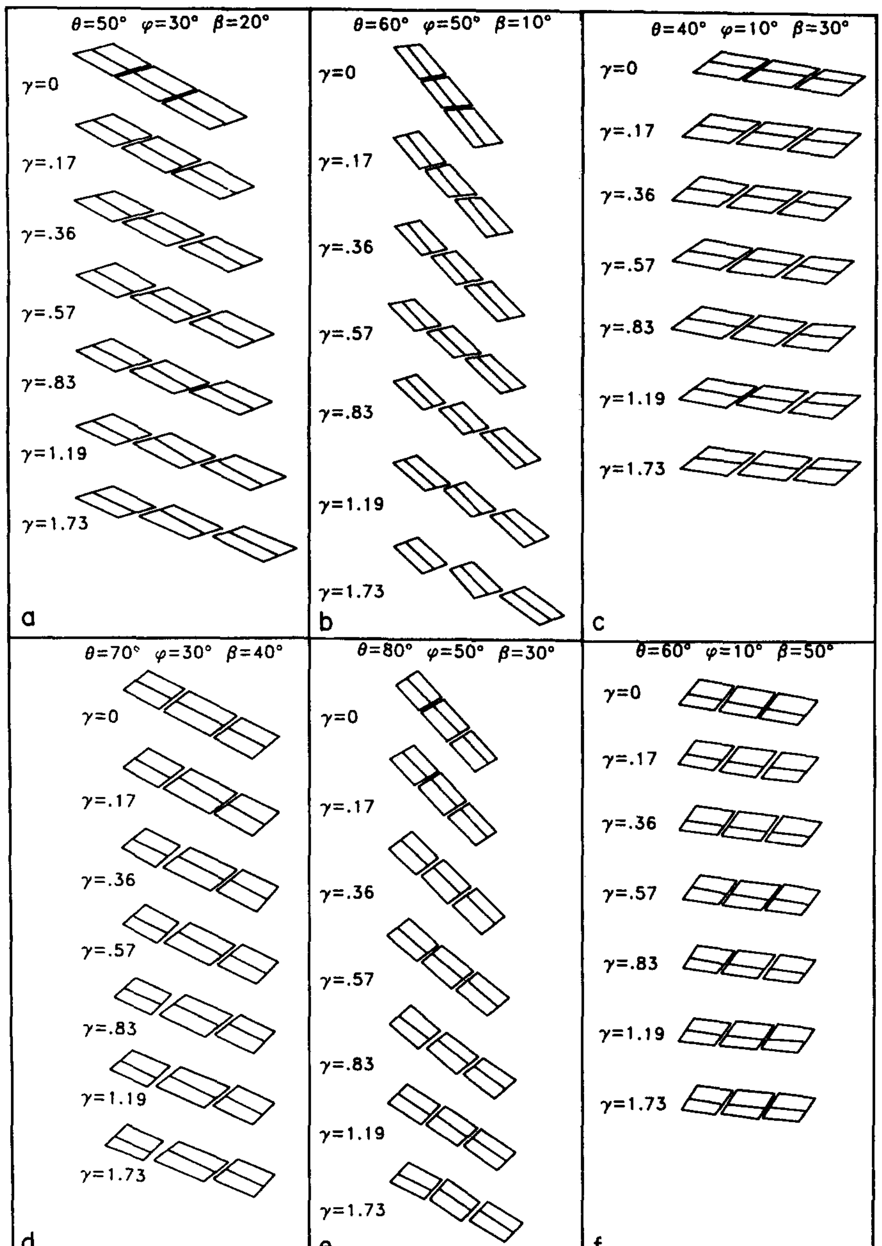

Fig. 9. Results of typical model experiments which illustrate the effect of varying the angle between 'fractures' and the shear zone boundary on the evolution of type III asymmetric boudinage. All experiments are the same scale and the shear plane is oriented E–W vertical.

ing, lower angles between fractures and the shear zone boundary results in greater amounts of displacement between blocks and more extension of layering (Figs. 9a & d, b & e, c & f). For experiments in which the angle between fractures and the shear zone boundary (β) are similar but the orientation of layering varies, similar amounts of displacement between blocks and extension of layering have occurred (Figs. 9c & e). Those experiments which experienced the most displacement and extension of layering were those with the lowest βs.

The amount of shear strain for planes within a shear zone is dependent on their orientation (Ramsay & Huber 1983) and it appears that fractures oriented such that they experience high shear strain are those that experience the most displacement, regardless of the orientation of layering in the shear zone. However, the angle between layering and the shear zone boundary can also be significant. For example, a series of experiments were run with layering parallel to the shear zone boundary, an orientation for which no extension of layering would be expected. For all orientations of fractures in those layers, no displacement or extension occurred. For layers oriented such that shortening would be expected (Figs. 10c & d), slip on fractures was such that shortening was accommodated. The angle between layering and fractures can also have an effect on block rotation despite the orientation of layering in the shear zone. For layers with fractures inclined at 90° to layering (θ) (Fig. 10b), blocks separated and rotated in harmony with the sense of displacement across the model for all orientations of layering consistent with extension. An additional interesting result of the model studies is their departure from some theoretical predictions. Ghosh & Ramberg (1976) showed that for angles lower than 45° to the shear zone boundary, a low aspect ratio inclusion should rotate faster than a long aspect ratio inclusion or a passive marker line. Thus, for models with ϕ less than 45°, one would expect individual boudins to rotate faster than the line connecting their centers. This does not occur in the models (Figs. 9a & d) suggesting that shear between boudins affects their rate of rotation. Thus, the model studies which show that type III boudins rotate at a lower rate than layering (Figs. 7 and 9) help explain the apparent 'back rotation' of boudins observed in the field (Figs. 4 and 5).

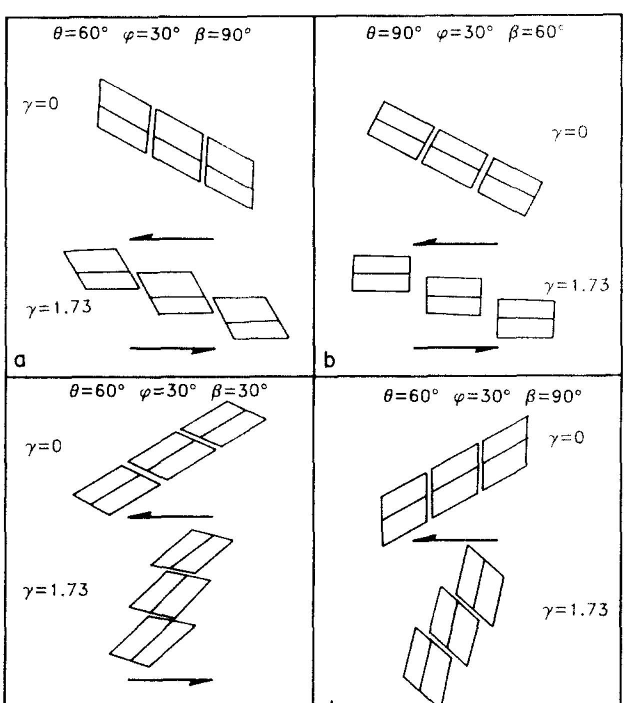

Fig. 10. Results of typical model experiments designed to study the effect of varying the angle between the layering and the shear zone boundary.

DISCUSSION AND CONCLUSIONS

Field and model studies suggest that, in addition to the two types of asymmetric boudinage noted by Hanmer (1986), there is a third mechanism that can produce asymmetric boudinage with similar shapes. These boudins, termed type III asymmetric boudins, form as a result of layering lying within the extensional field of a shear zone. There are two possible origins for the fractures which must be present in order for this type of boudinage to form. If the ductility contrast between layers is large, fracturing of the competent layer could occur during shearing. This appears to be the case for the field example but is difficult to prove. Extension fractures formed during shearing will always be inclined to the shear zone such that boudins similar to those depicted in Fig. 9 result. Strömgård (1973) has suggested that boudins formed at high confining pressure would only be rhomboidal under conditions of high differential stress and such stress states would be expected for shear zones. Different angles between layering and extensional fractures would result from different amounts of differential stress (Strömgård 1973). The origin of extension fractures is of particular interest if they can be related to the shear deformation. However, in general this is difficult to do because of the multiple deformation common in orogenic interiors where large mylonite zones commonly occur. Mineral filled fractures could be of pre-shearing origin and, in this case, a wide variety of angular relationships will be possible (e.g. Fig. 10). Gaudemer & Tapponier (1987) have suggested that fractures which are integral to the formation of type III boudinage may initiate as shear (mode II) fractures. The resulting shapes of the boudins they describe are very similar to those described here and, thus, their mechanism is interpreted to be essentially identical to a type III mechanism.

Hanmer (1986) has suggested that type II asymmetric boudinage could be used as a kinematic indicator in sheared rocks. Type II boudins require the pre-shearing presence of pinch and swell boudins lying parallel to the shear zone boundary (Hanmer 1986). After even moderate shear strains, it will be difficult to determine if boudins were of pre-shearing origin or were produced during shearing. Additionally, it will be difficult to know if layering was parallel to the shear zone boundaries. If the fractures required for type III asymmetric boudinage are produced during shearing (Fig. 9), type II and type III asymmetric boudins will appear the same and the kinematic interpretation based on either mechanism will be identical. However, in some instances the shapes of the asymmetric boudins could be opposite to that expected for the shear sense and one could misinterpret the sense of shear. For example, given the pre-shearing geometry shown in Fig. 10(a), a dextral shear sense could be deduced if one assumed a type II mechanism. At high shear strains the enveloping surface of layering would appear parallel to the shear zone and the pre-shearing geometry would be difficult to interpret. If one can determine the shear sense through independent means, the sense of type III boudin asymmetry will be useful in determining the pre-shearing geometry of layering and fractures.

There are several criteria which might be used to distinguish type II from type III asymmetric boudins. Type III boudins should display a clear truncation of any internal fabric of the boudinaged layer whereas type II should not. Identifiable vein filling in the 'tails' of the boudin will also be a strong indication of a type III mechanism although intra-boudin mineralization is also common. An additional type of asymmetric boudinage may develop in shear zones and has not been investigated in this study. For layered sequences with moderate ductility contrasts, shearing may result in asymmetric pinch and swell boudins formed as a result of the extension direction being non-parallel to layering. Thus, at least four types of asymmetric boudinage may develop in shear zones depending on the pre-shearing geometries and the relative ductilities between layers. Care should be taken to determine the mechanism of boudinage and as many aspects of the pre-shearing geometry before using asymmetric boudinage as a kinematic indicator.

Acknowledgements—The work described in this paper was supported by grants from the Research Corporation, The National Science Foundation (grant number 87-08244), the Colgate University Research Council and the Connecticut Geology and Natural History Survey. Field and laboratory support was supplied by Elizabeth Rodman and Chris Vhynal. Discussions with W. Means, J. Bursnall and J. McLelland have been of immeasurable value to the author as have been comments on an early version of this paper by S. Hanmer and two anonymous reviewers. The simple shear device was built by H. Kutzuba.

REFERENCES

Cloos, H. 1947. Boudinage. *Trans. Am. geophys. Un.* **28**, 626–632.

Dixon, H. R. 1982. Multistage deformation of the Preston Gabbro, eastern Connecticut. In: *Guidebook for Fieldtrips in Connecticut and South-central Massachusetts* (edited by Joesten, R. & Quarrier, S.). Connecticut Geological and Natural History Survey, Guidebook No. 5, 453–463.

Fullagar, P. K. 1980. A description of nucleation of folds and boudins in terms of vorticity. *Tectonophysics* **65**, 39–55.

Gaudemer, Y. & Tapponier, P. 1987. Ductile and brittle deformations in the northern Snake Range, Nevada. *J. Struct. Geol.* **9**, 159–180.

Ghosh, S. K. & Ramberg, H. 1976. Reorientation of inclusions by combinations of pure and simple shear. *Tectonophysics* **34**, 1–70.

Goldstein, A. G. 1982. Geometry and kinematics of ductile faulting in a portion of the Lake Char mylonite zone, Massachusetts and Connecticut. *Am. J. Sci.* **282**, 1378–1405.

Goldstein, A. G. 1986. A summary of fault motion histories for southeastern New England (abs.). *Geol. Soc. Am. Abs. w. Prog.* **18**, 19.

Goldstein, A. G. & Owens, J. 1985. Mesoscopic and microscopic structure of the Lake Char-Honey Hill mylonite zone. In: *Guidebook for Fieldtrips in Connecticut and Adjacent Portions of New York and Rhode Island* (edited by Tracey, R. J.). Connecticut Geological and Natural History Survey Guidebook No. 6, 159–183.

Hanmer, S. 1986. Asymmetrical pull-aparts and foliation fish as kinematic indicators. *J. Struct. Geol.* **8**, 111–122.

Hansen, E. 1971. *Strain Facies*. Springer Verlag, New York.

Lloyd, G. E. & Ferguson, C. C. 1981. Boudinage structures: some new interpretations based on elastic-plastic finite element simulations. *J. Struct. Geol.* **3**, 117–128.

Lloyd, G. E., Ferguson, C. C. & Reading, K. 1982. A stress transfer model for the development of extension fracture boudinage. *J. Struct. Geol.* **4**, 355–372.

Lundgren, L. W. & Ebblin, C. 1973. Honey Hill fault in eastern Connecticut: regional relations. *Bull. geol. Soc. Am.* **83**, 2773–2794.

O'Hara, K. & Gromet, L. P. 1983. Textural and Rb–Sr isotopic evidence for late Paleozoic mylonitization within the Honey Hill fault zone, southeastern Connecticut. *Am. J. Sci.* **283**, 762–779.

Ramberg, H. 1955. Natural and experimental boudinage and pinch-and-swell structures. *J. Geol.* **63**, 512–526.

Ramsay, J. G. 1967. *Folding and Fracturing of Rocks*. McGraw-Hill, New York.

Ramsay, J. G. & Huber, M. I. 1983. *The Techniques of Modern Structural Geology*. Volume I: *Strain Analysis*. Academic Press, New York.

Rast, N. 1956. The origin and significance of boudinage. *Geol. Mag.* **93**, 401–408.

Simpson, C. & Schmid, S. 1983. An evaluation of criteria to deduce the sense of movement in sheared rocks. *Bull. geol. Soc. Am.* **94**, 1281–1288.

Smith, R. B. 1975. Unified theory for the onset of folding boudinage and mullion structure. *Bull. geol. Soc. Am.* **86**, 1601–1609.

Smith, R. B. 1977. Formation of folds, boudinage and mullions in non-Newtonian materials. *Bull. geol. Soc. Am.* **88**, 312–320.

Strömgård, K. E. 1973. Stress distribution during deformation of boudinage and pressure shadows. *Tectonophysics* **16**, 215–248.

Wilson, G. 1982. *Introduction to Small-scale Geological Structures*. Allen, George & Unwin, London.